Free-free transitions of e-H system inside a dense plasma irradiated by a laser field at very low incident electron energies

A.K. Bhatia[1] and C. Sinha[2]
[1]*Solar Physics Laboratory, NASA/Goddard Space Flight Center, Greenbelt, MD 20771, USA*
[2]*Theoretical Physics Department, Indian Association for the Cultivation of Science, Jadavpur, Kolkata 700032, India*

The free-free transition is studied for an electron-hydrogen in the ground state at low incident energies in the presence of an external homogenous, monochromatic, and linearly polarized laser-field inside a hot dense plasma.The effect of plasma screening is considered in the Debye-Hückel approximation. The calculations are performed in the soft photon limit, assuming that the plasma frequency is much higher than the laser frequency. The incident electron is considered to be dressed by the laser field in a nonperturbative manner by choosing the Volkov solutions in both the initial and final channels. The space part of the scattering wave function for the electron is solved numerically by taking into account the electron exchange. The laser-assisted differential and total cross sections are calculated for single-photon absorption /emission and no photon exchange in the soft photon limit, the laser intensity being much less than the atomic field intensity. The calculations have been carried out for various values of Debye parameter, ranging from 0.005 to 0.12. A strong suppression is noted in the laser-assisted cross sections as compared to the field-free situation. A significant difference is noted for the singlet and triplet cross sections. The suppression is much more in the triplet states.

I. INTODUCTION

In recent years much attention is being paid to the atomic processes of different atomic systems embedded in a plasma. The motivations for such studies are manifold and were already emphasised in earlier works [1- 10] (and further References cited therein). The purpose of the present work is to study the influence of an external laser field on the free free transition process of electron - hydrogen system in a dense and hot plasma environment. Such studies have direct relevance to many real physical objects, e.g., laser produced plasma [7], fusion plasma confinement, high power gas lasers etc. In particular, the inverse bremstrahlung process is believed to play an important role in the breakdown and the heating process of a plasma illuminated by a laser beam [10]. The interpretation of the line emission from a dense high temperature plasma requires a detailed knowlege of spectroscpic as well as the collisional properties (e.g., collision strength, cross sections etc.) of the plasma constituents. However not much is known about the combined effects of plasma and laser field on the important collision processes [7, 10]. When a dense plasma is irradiated with an external laser field, the electromagnetic wave will not propagate through the plasma in the nonrelativistic case, if the plasma frequency is much higher than the frequency of the electromagnetic wave. However, still there will

be transfer of energy from the laser to the plasma without altering the average plasma properties [11].

Inside a dense plasma, partial shielding by the neighbouring charged particles weakens the pure coulomb interaction between two charged particles at large separations, thereby affecting the collision cross sections. It is therefore expected that the effect of plasma screeining on the collision cross sections should be particularly large at low incident energies [6].

In most of the collisional experinents with or without the presence of laser field, the plasma environment is always present to some extent and it can significantly affect the collision process. It is therefore desirable and quite worthwhile to study the atomic collision processes under the combined presence of the plasma and the laser field. Now a days by virtue of the rapid and dynamic development in the laser technology, laser assisted collision experiments are becoming incresingly feasible at laboratories following which a significant number of theoretical studies were performed for different atomic collision processes. Laser assisted excitation, ionisation, recombination and the free- free transition processes are the basic underlying mechanisms for different highly nonlinear phenomena, e.g., nonsequential double or multiple ionisation (NSDI, NSMI), high harmonic generation (HHG) and high order above threshold ionisation (HATI) that occur when atomic or molecular targets are irradiated with strong and short wave length laser field. The Coulomb potential of the system is distorted by such field and as a result, the electron can escape from the atoms (or molecules) through tunneling. If the tunneled electron driven by the laser field revisits its parent atomic ion during the reverse cycle of the laser field, the electron again may either be elastically scattered off its parent ion leading to HATI peaks or it can recombine with it generating a high order harmonic (HHG). The tunneled electron can also reionise the residual nucleus leading to NSDI. It is therefore expected that the laser assisted collisional experiments where the collision partners are under full control could provide detailed insight into the above phenomena.

Apart from these, the laser assisted electron- atom collisions allow on the one hand the experimental observation of different multiphoton processes [12- 16] at relatively moderate laser field intensities while on the other hand it allows to measure some electron-atom scattering parameters which otherwise would not be accessible to experiments. In view of the recent availability of the tunable lasers with a wide frequency range, unique effects can be observed which are not present in ordinary electron-atom scattering.

In a recent work [17], we investigated the effect of an external laser field on the scattering of low energy electrons from a ground state hydrogen atoms in a gaseous medium. Wallbank and Holmes [15] carried out experiments on the scattering of low energy electrons from He atoms in the presence of a pulsed CO_2 laser with the laser polarization parallel to the momentum transfer and the photon energy being 0.117 eV. Our results for the H atom [17] were found to be in accord with the experiment [15] qualitatively.

The present work addresses the laser assisted free free (FF) transition of a plasma embedded electron – hydrogen (ground state) system at very low incident energies in the frame work of Debye Hückel model [18].

Theory:

The free-free transition in the presence of an external laser field is given by

$\omega(l) + e^-(k_i) + H(1s) \rightarrow e^-(k_f) + H(1s)$, **(1)**

where l is the number of photon absorbed or emitted. The processes in which $l < 0$ and $l > 0$ correspond to stimulated brehmsstrahlung (emission) and inverse brehmsstrahlung (absorption), respectively, while $l=0$ corresponds to pure laser-assisted elastic (free-free) scattering; $\vec{k}_i$ and $\vec{k}_f$ being the incident and final momenta of the projectile electron.

The laser field is chosen to be homogeneous, monochromatic, and linearly polarized and is represented by $\vec{\varepsilon}(t) = \vec{\varepsilon}_0 \sin(\omega t + \xi)$, where ξ is the initial phase of the laser field, the corresponding vector potential in the dipole approximation is $\vec{A}(t) = \vec{A}_0 \cos(\omega t + \xi)$ with $\vec{A}_0 = c\vec{\varepsilon}_0 / \omega$, and ξ is chosen equal to zero in the present work. $\hat{\varepsilon}$ correspond to laser polarization, parallel to the incident electron momentum.

.

The total Hamiltonian of the system in the laser field is given by

$$H = -(i\nabla_1 + A)^2 - (i\nabla_2 + A)^2 + V_D \quad \textbf{(2)}$$

where V_D represents the Debye-Hückel potential [18] of the form:

$$V_D = -\frac{2Z}{r_1} e^{-\mu r_1} - \frac{2Z}{r_2} e^{-\mu r_2} + \frac{2}{r_{12}} e^{-\mu r_{12}}, \quad \textbf{(3)}$$

where $\vec{r}_1$ and $\vec{r}_2$ are the position vectors of the incident electron and the bound electron of the target hydrogen atom, r_{12} is the relative distance. The parameter μ is called the Debye screening parameter and is given by $\mu = [\frac{4\pi n (Ze)^2}{k_B T}]^{0.5}$, where n is the plasma density and T is the temperature of the plasma. The Debye length is given by 1/μ. We use Rydberg units throughout our calculations. Therefore, μ has the units of $1/a_0$, where a_0 is the Bohr radius of the hydrogen atom. For μ=0.1, we find $n/T = 9.04 \times 10^5$. At room temperature, T=300K, we find $n = 2.712 \times 10^8$ / cm^3. This is a very reasonable density at which most experiments could be carried out, because there is never a perfect vacuum. We have carried out calculations for μ=0.005 to 0.12 which is a very reasonable choice.

The energy of the laser field is ω= 0.0043 a.u. (1 a.u. being 5×10^9 V/cm) , i.e., we are dealing with soft photons and the strength of the laser field is $\in_0$ =0.01a.u (1a.u. being 10^{16} W/cm^2). The incident energy k_i^2 of the electron ranges from 0.01 to 0.64 Ry or from 0.136 to 8.707 eV in our calculation. This incident energy is very much below the 'n'=2 threshold of the hydrogen atom.

The energy conservation relation for this FF process is given by

$k_f^2 = k_i^2 + 2l\omega, \quad l=0, \pm1, \pm2, \ldots$ **(4)**

The transition matrix element for the laser-assisted process (2) is given by [17] :

$$T_{if} = -i\int dt < \psi_f \mid V_f \mid \Psi_i^+ > . \qquad \textbf{(5)}$$

where the perturbation

$$V_f = (\frac{2Z}{r_1} e^{-\mu r_1} - \frac{2}{r_{12}} e^{-\mu r_{12}}). \qquad \textbf{(6)}$$

The projectile electron is considered to be dressed by the laser field in a nonperturbative manner by choosing the Volkov solutions [19] in both the initial and final channels.

The final channel asymptotic wave function ψ_f in Eq. (5) satisfies the following Schrödinger equation:

$$[-(i\vec{\nabla}_1 + \vec{A})^2 - (i\vec{\nabla}_2 + A)^2 - \frac{2Z}{r_2} e^{-\mu r_2} - E]\psi_f = 0. \qquad \textbf{(7)}$$

In the present work, we have neglected the laser-target interactions as compared to the dominant projectile-target interactions at very low incident energies. Thus the final channel wave function ψ_f is chosen as

$$\psi_f = \chi_{k_f} \phi_f \qquad \textbf{(8)}$$

The final state wave function ϕ_f is the same as the initial state wave function ϕ_0 given in Eq. (24) and calculated in the presence of the Debye-Hückel [18] potential. The time dependent Schrödinger equation describing the electron in the laser field in the Coulomb gauge is given by

$$i\frac{\partial \chi_k^C(\bar{r},t)}{\partial t} = [-\nabla^2 + H\ (t)]\ \chi_k^C(\bar{r},t) \qquad \textbf{(9)}$$

The superscript ‘C’ indicates the Coulomb gauge and

$$H(t) = i\frac{2q}{c}\vec{A}(t).\vec{\nabla} + \frac{q^2}{c^2}A^2(t)\ . \qquad \textbf{(10)}$$

In the above equation q=-e is the charge on the projectile. The solution of Eq. (9) is given by the Volkov wavefunction [19- 21]

$$\chi_k^C(\vec{r},t) = (2\pi)^{-3/2} \exp(i\vec{k}\cdot\vec{r} - i[E_k t - \vec{\alpha}_0 \cdot \vec{k} \sin(\omega t - \delta)] \quad \textbf{(11)}$$

where $E_k = k^2$ is the free energy and

$$\vec{A}(t) = \vec{A}_0 \cos(\omega t - \delta), \vec{\alpha}_0 = \vec{\varepsilon}_0 / \omega^2 \quad \textbf{(12)}$$

Now, we use the generating function of the Bessel functions [20, 21]:

$$\exp(-k_i \alpha_0 \sin(\omega t) = \sum_{m=-\infty}^{\infty} \exp(im\omega t) J_m(-k_i \alpha_0). \quad \textbf{(13)}$$

Using the above generating function and in view of the relation

$$J_m(-z) = (-1)^m J_m(z), \quad \textbf{(14)}$$

Eq(11) can be recast as (the superscript being omitted)

$$\chi_{k_i}(r,t) = (2\pi)^{-3/2} \sum (-i)^m J_m(k_i \alpha_0) \exp\{i[\vec{k}\cdot\vec{r} - (E_{k_i} - m\omega)t]\}. \quad \textbf{(15)}$$

The full scattering wave function Ψ_i^+ in the initial channel satisfies the three-body Schrödinger equation, obeying the incoming wave boundary condition**:**

$$(H - E)\Psi_i^+ = 0. \quad \textbf{(16)}$$

Now the spatial part ($\Psi_s(\vec{r}_1,\vec{r}_2)$ of the full scattering wave function Ψ_i^+ is obtained numerically in the framework of the partial wave expansion by solving the initial channel Schrödinger equation, incorporating the electron exchange [22]. Finally, T_{if} reduces to

$$T_{if} = \frac{-i}{(2\pi)^{1/2}} \sum \delta(E_{k_f} - E_{k_i} + l\omega) J_l(\vec{q}.\vec{\alpha}_0) I, \quad \textbf{(17)}$$

where $\vec{q} = \vec{k}_i - \vec{k}_f$ is the momentum transfer and *I* is the space part of the transfer matrix element and is given by

$$I = \int\int d^3 r_1 d^3 r_2 \exp(i\vec{k}_f.\vec{r}_1) \phi_0(\vec{r}_2)\, V_f(\vec{r}_1,\vec{r}_2) \Psi_i^+(\vec{r}_1,\vec{r}_2). \quad \textbf{(18)}$$

In the weak field limit (i.e., neglecting the target dressing effect), the laser-assisted differential cross section (DCS) for the elastic scattering, for *l* photons, can be related to the field free (FF) differential cross section by the relation [17, 19 -21]

$$[d\sigma^{l}(k_i, k_f(l))/d\Omega]_{laser} = (k_f(l)/k_i)\, J_l^2(\mathbf{q}.\alpha_0)\, [d\sigma^{l}/d\Omega]_{FF,} \qquad \textbf{(19)}$$

where $[d\sigma^{l}/d\Omega]_{FF}$ is the field-free elastic cross section, J_l are the Bessel functions of integer order l, $\vec{q} = \vec{k}_f - \vec{k}_i$ is the momentum transfer, $\boldsymbol{k}_i$, $\boldsymbol{k}_f$ are the initial and final momenta of the electron.

The above relation, given in Eq. (19) is called the so called Kroll-Watson [19] Approximation (KWA). In order to calculate the field-free [FF] elastic differential and total cross sections, we carry out the calculation of phase shifts in the exchange approximation [22].

The ground state wave function of the target H atom gets dressed under the Debye-Hückel [18] potential and is given by

$$\phi_0 = e^{-ar} \sum_i C_i r^i \qquad \textbf{(20)}$$

Since the lowest term does not contain r, the summation index ranges from 0 to N=14, i.e., we have 15 terms in the expansion. The corresponding ground state energy is calculated variationally by using

$$< \phi_0 \mid -\nabla_2^2 - \frac{2Z}{r_2} e^{-\mu r_2} \mid \phi_0 >= E_0 \phi_0 . \qquad \textbf{(21)}$$

We find that the energy is not sensitive to the variation of the nonlinear parameter a in the expansion given in Eq. (20) and as such we kept it fixed at 1.0. The ground state energies for various values of the Debye parameter are given in Table I.

Table I. Ground state energies of the hydrogen atom for various values of μ with 15 terms in the expansion of the wave function (20).

Debye parameter μ	E(Ry)	
0.0	-1.00	
0.005	-9.90[-1]	
0.01	-9.80[-1]	
0.015	-9.70[-1]	
0.02	-9.61[-1]	
0.04	-9.22[-1]	
0.08	-8.49[-1]	
0.12	-7.80[-1]	

As μ increases, the ground state energy moves towards the continuum. Finally, for large values of μ the atom becomes unbound.

The wave function ($\Psi_s(\vec{r}_1,\vec{r}_2)$ for the scattering in the exchange approximation [22] is given by

$$\Psi_s(\vec{r}_1,\vec{r}_2) = u(\vec{r}_1)\phi_0(\vec{r}_2) \pm (1 \leftrightarrow 2), \quad \textbf{(22)}$$

where $u(\vec{r}) = \frac{u(r)}{r} Y_{L0}(\Omega)$ **(23)**

The upper sign (+) refers to singlet states and the lower sign (-) to triplet states. The equation for the scattering function u(r) is obtained from

$$< \phi_0(\vec{r}_2) \mid H^{'} - E \mid \Psi(\vec{r}_1,\vec{r}_2) >= 0 \quad \textbf{(24)}$$

The Hamiltonian in the above equation is given by

$$H^{'} = -\nabla_1^2 - \nabla_2^2 + V_D \quad \textbf{(25)}$$

Carrying out the integration leads to the scattering equation for *u(r),* by letting $r_1 = r$, we obtain

$$[\frac{d^2}{dr^2} - \frac{l(l+1)}{r^2} + \frac{2Z}{r} e^{-\mu r} - V_3(r) + k^2]u(r) \pm \{r\phi_0(r)\delta_{l0}F_1 - \frac{2}{(2l+1)}\phi_0(r)[\frac{e^{-\mu r}}{r^l}F(r) + r^{l+1}e^{\mu r}G(r)]\} = 0,$$

(26)

where

$$F_1 = \int_0^{\alpha} dx B(x)u(x) \quad \textbf{(27)}$$

$$F(r) = \int_0^{r} dx\, x^{(l+1)} e^{\mu x}\phi_0(x)u(x) \quad \textbf{(28)}$$

$$G(r) = \int_r^{\alpha} \frac{e^{-\mu x}}{x^l}\phi_0(x)u(x) \quad \textbf{(29)}$$

$$B(x) = \sum_j C_j[\, j(j-1)x^{j-2} - 2ajx^{j-1}] + 2Ze^{-\mu x}\phi_0(x) + (k^2 + a^2)x\phi_0(x) \quad \textbf{(30)}$$

$$V_3(r) = \sum_j C_j \sum_i C_i [\frac{e^{-\mu r}}{r}\{\frac{(j+i)!}{q^{j+i+1}} - e^{-qr}v(r,q)\} + e^{\mu r}e^{-pr}w(r,p)], \quad \textbf{(31)}$$

where, $q=2a-\mu$ **and** $p=2a+\mu$.

$$v(r,q)=\sum_{s}^{i+j}\frac{(i+j)!}{(i+j-s)!}\frac{r^{i+j-s}}{q^{1+s}},$$

and

$$w(r,p)=\sum_{s}^{i=j-1}\frac{(i+j-1)!}{(i+j-1-s)!}\frac{r^{i+j-1-s}}{p^{1+s}}$$

In Eqs. (26 - 27), the minimum value of 's'=0. Because of the parameter μ, the resulting integro-differential equation is quite different from the well known exchange approximation equation [22]. However, when we put μ=0, a=Z=1 and N=1 in Eq. (30), we recover the equation given in [22] for the exchange approximation.

We have solved the resulting equation for l=L=0 to 7, numerically by the noniterative method. The phase shifts obtained have the variational lower bounds and they are calculated from the function $u(r)$,

$$u(r)=A\sin(kr-\frac{L\pi}{2}+\eta)\quad for\ r\to\infty \qquad (\mathbf{32})$$

A better approximation for higher partial waves would have been the use of the Method of Polarized Orbitals [23]. Since the ground state wave function is rather complicated, the polarized orbital function $u_{1s\to p}$ [23] has to be obtained numerically for each partial wave L. This would have made the problem quite cumbersome to solve. Moreover, the long-range polarization potential arises from the expansion of $1/r_{12}$. Because of the nonlinear parameter μ in the term $\exp[-\mu r_{12}]/r_{12}$, this term will not contribute when r_1 *or* r_2 goes to infinity in the expansion of $1/r_{12}$. This shows that there will not be any long-range potential in this problem.

Similarly, the calculations that include correlations [24] would be too much involved. At present, our main interest is to see the behavior of the cross sections in the combined effect of the laser field and the Debye-Hückel potential.

The phase shifts, for singlet and triplets states have been calculated for the partial waves [L=0 to7] for the values of μ given in Table I. The results in the Table are accurate up to the figures quoted. The field free (FF) elastic differential cross section (DCS) is given by [17] :

$$\mathbf{[d\sigma^{l}/d\Omega]_{FF}=(1/k_i^2)\left|\sum(2L+1)\exp[i\delta_L]\sin(\delta_L)P_L(\cos\theta)\right|^2,} \qquad \mathbf{(33)}$$

where ϑ is the scattering angle between r and the Z axis.

Results & Discussions:

We have computed the laser assisted (LA) Free – Free transitions (both differential and total cross sections) of a H atom embedded in a dense plasma under the Debye Hückel potential [18]. Tables II and III demonstrate the present LA total free – free transition cross sections (TCS) for the incident k=0.1, 0.2, 0.3, 0.5 and 0.8 in both the triplet and singlet states for various values of the parameter μ along with the corresponding field-free (FF) cross sections. We also provide the results obtained by us [17] in the absence of the Debye-Hückel potential. We note that the cross sections change significantly when the irradiated system is embedded in a Debye plasma. As μ increases from the zero value , the cross sections increase remarkably in all the cases (l=-1, 0, 1) up to μ=0.02 while beyond that they start to decrease. In all the cases the cross sections are very much suppressed compared to the FF values.

Table II. Comparison of the triplet cross sections with FF cross sections for electron-hydrogen scattering for various values of μ.

Parameter μ	K	l=-1	l=0	l=1	Field Free
0.00[a]	0.1	1.14[-1]	8.21[-1]	1.15	5.15[+1]
	0.2	1.72[-1]	3.51[-1]	4.32[-1]	5.52[+1]
	0.3	1.35[-1]	2.40[-1]	2.60[-1]	5.49[+1]
	0.5	1.55[-1]	3.29[-1]	3.19[-1]	4.87[+1]
	0.8	1.51[-1]	3.42[-1]	3.24[-1]	3.07[+1]
0.00	0.1	1.55[-1]	1.41	1.77	6.79[+1]
	0.2	2.36[-1]	6.35[-1]	7.26[-1]	6.28[+1]
	0.3	1.71[-1]	3.50[-1]	3.79[-1]	5.64[+1]
	0.5	1.09[-1]	1.99[-1]	2.00[-1]	4.30[+1]
	0.8	8.14[-2]	1.58[-1]	1.54[-1]	2.55[+1]
0.005	0.1	4.75	4.77[+2]	2.75[+1]	1.14[+3]
	0.2	2.55	4.37[+1]	8.65	2.13[+2]
	0.3	1.40	9.57	4.42	9.81[+1]
	0.5	3.06[-1]	1.08	7.81[-1]	4.81[+1]
	0.8	6.71[-2]	1.31[-1]	1.22[-1]	2.50[+1]
0.01	0.1	8.51	8.45[+2]	5.29[+1]	2.08[+3]
	0.2	5.31	9.35[+1]	1.85[+1]	3.92[+2]
	0.3	3.03	2.18[+1]	9.77	1.54[+2]
	0.5	6.69[-1]	2.66	1.86	5.79[+1]
	0.8	9.96[-2]	2.68[-1]	2.29[-1]	2.59[+1]
0.015	0.1	9.82	9.37[+2]	6.84[+1]	2.48[+3]
	0.2	7.32	1.27[+2]	2.65[+1]	5.22[+2]

	0.3	4.42	3.19[+1]	1.45[+1]	2.03[+2]
	0.5	1.04	4.28	2.96	6.80[+1]
	0.8	1.48[-1]	4.58[-1]	3.84[-1]	2.74[+1]
0.02	0.1	9.86	8.89[+2]	7.84[+1]	2.58[+3]
	0.2	8.63	1.45[+2]	3.25[+1]	6.08[+2]
	0.3	5.49	3.96[+1]	1.82[+1]	2.42[+2]
	0.5	1.39	5.76	4.00	7.74[+1]
	0.8	2.02[-1]	6.66[-1]	5.54[-1]	2.90[+1]
0.04	0.1	7.33	4.89[+2]	9.23[+1]	2.17[+3]
	0.2	9.88	1.44[+2]	4.28[+1]	7.11[+2]
	0.3	7.46	5.15[+1]	2.59[+1]	3.23[+2]
	0.5	2.39	9.80	7.00	1.06[+2]
	0.8	4.16[-1]	1.46	1.22	3.53[+1]
0.08	0.1	3.99	1.51[+2]	7.13[+1]	1.33[+3]
	0.2	7.36	7.89[+1]	3.72[+1]	6.04[+2]
	0.3	6.56	4.02[+1]	2.41[+1]	3.28[+2]
	0.5	3.03	1.20[+1]	8.89	1.28[+2]
	0.8	7.10[-1]	2.49	2.10	4.39[+1]
0.12	0.1	2.52	6.59[+1]	4.69[+1]	8.96[+2]
	0.2	5.10	4.22[+1]	2.69[+1]	4.82[+2]
	0.3	4.98	2.72[+1]	1.87[+1]	2.95[+2]
	0.5	2.82	1.07[+1]	8.23	1.30[+2]
	0.8	1.71	5.50	4.80	1.18[+2]

a. These the results are obtained without the Debye potential and using very accurate phase shifts, which include the contribution of short and long range correlations.

Table III. Comparison of the singlet cross sections with FF cross sections for electron-hydrogen scattering for various values of μ.

Parameter μ	K	L=-1	l=0	L=1	Field Free
0.00[a]	0.1	8.81[-1]	7.85	1.01[+1]	3.87[+2]
	0.2	9.68[-1]	2.90	3.10	2.43[+2]
	0.3	5.03[-1]	1.13	1.21	1.38[+2]
	0.5	1.30[-1]	2.59[-1]	2.55[-1]	4.15[+1]
	0.8	3.35[-2]	7.79[-2]	7.25[-2]	1.04[+1]
0.00	0.1	1.33	1.26[+1]	1.56[+1]	5.79[+2]
	0.2	1.18	3.43	3.88	2.87[+2]
	0.3	5.12[-1]	1.15	1.24	1.39[+2]

	0.5	9.48[-2]	1.69[-1]	1.70[-1]	3.77[+1]
	0.8	9.29[-3]	1.40[-2]	1.39[-2]	8.02
0.005	0.1	6.21	5.11[+2]	4.36[+1]	1.73[+3]
	0.2	3.30	4.35[+1]	1.09[+1]	4.26[+2]
	0.3	1.45	8.50	4.11	1.72[+2]
	0.5	2.68[-1]	9.57[-1]	6.74[-1]	4.26[+1]
	0.8	4.38[-2]	1.43[-1]	1.20[-1]	9.18
0.01	0.1	9.88	8.62[+2]	7.15[+1]	2.65[+3]
	0.2	5.78	8.92[+1]	1.94[+1]	5.88[+2]
	0.3	2.84	1.92[+1]	8.46	2.19[+2]
	0.5	6.09[-1]	2.47	1.68	5.21[+1]
	0.8	1.12[-1]	3.93[-1]	3.29[-1]	1.15[+1]
0.015	0.1	1.11[+1]	9.39[+2]	8.74[+1]	3.01[+3]
	0.2	7.51	1.19[+2]	2.60[+1]	7.01[+2]
	0.3	4.02	2.81[+1]	1.23[+1]	2.60[+2]
	0.5	9.61[-1]	4.28	2.72	6.19[+1]
	0.8	1.89[-1]	6.72[-1]	5.62[-1]	1.40[+1]
0.02	0.1	1.10[+1]	8.79[+2]	9.62[+1]	3.08[+3]
	0.2	8.56	1.34[+2]	3.06[+1]	7.71[+2]
	0.3	4.91	3.47[+1]	1.53[+1]	2.91[+2]
	0.5	1.29	5.41	3.69	7.09[+1]
	0.8	2.66[-1]	9.52[-1]	7.97[-1]	1.66[+1]
0.04	0.1	8.10	4.54[+2]	9.95[+1]	2.16[+3]
	0.2	8.94	1.25[+2]	3.59[+1]	8.12[+2]
	0.3	6.36	4.40[+1]	2.10[+1]	3.45[+2]
	0.5	2.21	9.27	6.46	9.69[+1]
	0.8	5.48[-1]	1.95	1.64	2.60[+1]
0.08	0.1	1.85	9.84[+1]	3.00[+1]	5.88[+2]
	0.2	5.23	5.71[+1]	2.33[+1]	5.81[+2]
	0.3	5.14	3.27[+1]	1.81[+1]	3.10[+2]
	0.5	2.73	1.11[+1]	8.06	1.13[+2]
	0.8	8.99[-1]	3.13	2.67	3.83[+1]
0.12	0.1	1.77	5.55[+1]	3.58[+1]	5.96[+2]
	0.2	2.52	4.23[+1]	1.23[+1]	3.02[+2]
	0.3	3.38	1.97[+1]	1.24[+1]	2.39[+2]
	0.5	2.48	9.70	7.31	1.09[+2]
	0.8	1.03	3.52	3.02	4.39[+1]

a. These the results are obtained without the Debye potential and using very accurate phase shifts, which include the contribution of short and long range correlations.

The overall accuracy of the reults in Tables II & III is within 10%. We note from the Tables that as as μ increases from zero, the cross sections initially increase upto a certain value of μ and beyond that (~ μ = 0.02) they decrease. The laser assisted cross sections are suppressed as compared to the FF ones and the suppression is more for the triplet cross sections than for the singlet ones.

Figures 1- exhibit the effect of the laser field on the field free plasma embedded cross sections . Fig. 1 displays the LA singlet TCS for the cases of single-photon emission (l=-1), no photon transfer (l= 0) and single-photon absorption (l=1) with an incident momentum k_i=0.1. As may be noted, the cross section has a prominent peak around μ=0.02 , the peak value being dependent on the value of l. Cross sections decrease very rapidly as μ increases up to a value ~ 0.8 beyond which the TCS becomes almost independent of μ. For low incident energies (k_i = 0.1), the peak of the TCS occurs at a much lower value of μ, i.e., for a larger value of the Debye length indicating that the projectile elctron is moving in an almost pure coulombic potential.

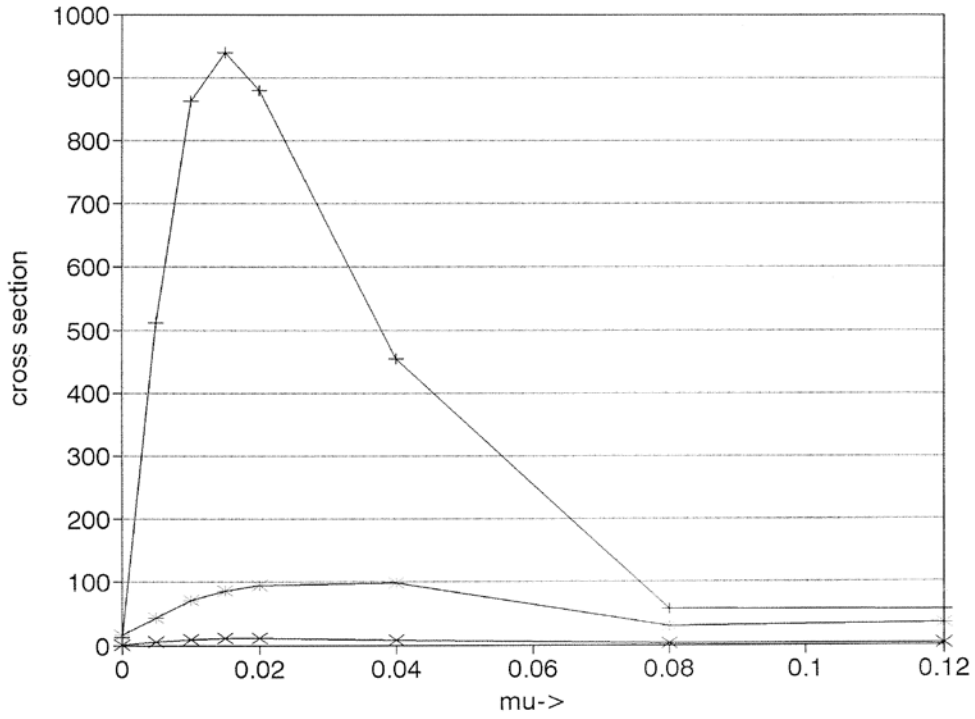

Fig.1. (color online only)Total cross sections (TCS) vs μ in atomic unit (a.u.) for singlet, k=0.1 . The upper curve is for (l=0), the middle curve is for single photon absorption (l=1) and the lowest one is for emission (l=-1).

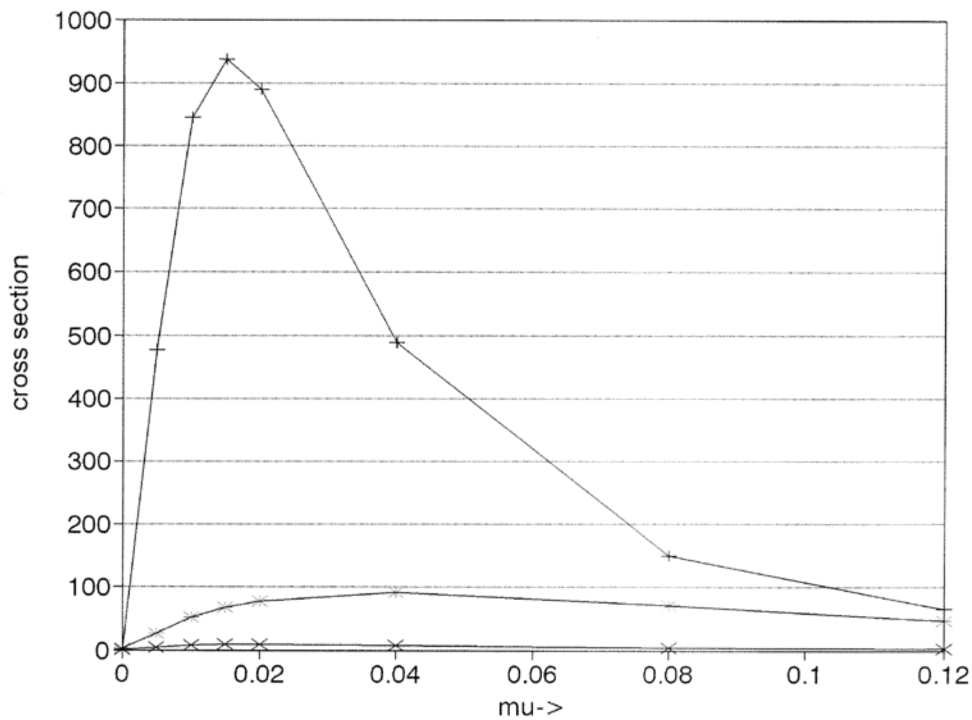

Fig.2. (color online only)Total cross secions (TCS) vs μ in a.u. for triplet, k=0.1. The upper curve is for (l=0), the middle curve is for single photon absorption (l=1), and the lowest one is for single photon emission (l=-1).

Fig. 2 reveals the same behavior as is observed in the triplet case for k_i=0.5.

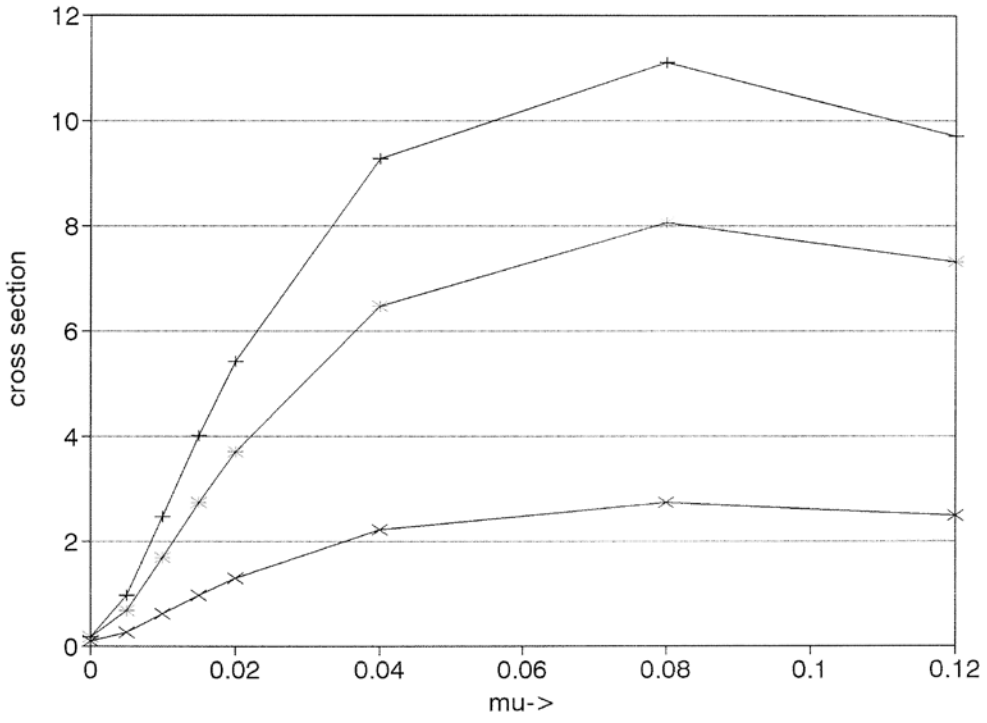

Fig.3. (color online only) TCS vs μ in a.u. for singlet, k=0.5. The upper curve is for l=0,the middle curve is for l=1 and the lower curve is for l=-1.

Fig. 3 reveals the effect of the laser field and the Debye-Hückel potential on the TCS for a single-photon emission (l=-1), no photon transfer (0) and a single photon absorption (1) with an incident k_i=0.5 in the singlet state. The cross section (TCS) is found to rise gradually and have peaks at around $\mu = \sim 0.08$ beyond which it falls off very slowly and become almost constant for higher valus of μ. The cross sections are smaller in magnitude as compared to those for k_i=0.1 as expected. The peak value of the TCS occurs at a much higher value of μ (compare Figs. 1 & 3) i.e., at a lower Debye length for higher incident energy indicating that the Debye screening increases with increasing incident energy since in this case the incident electron moves closer to the target.

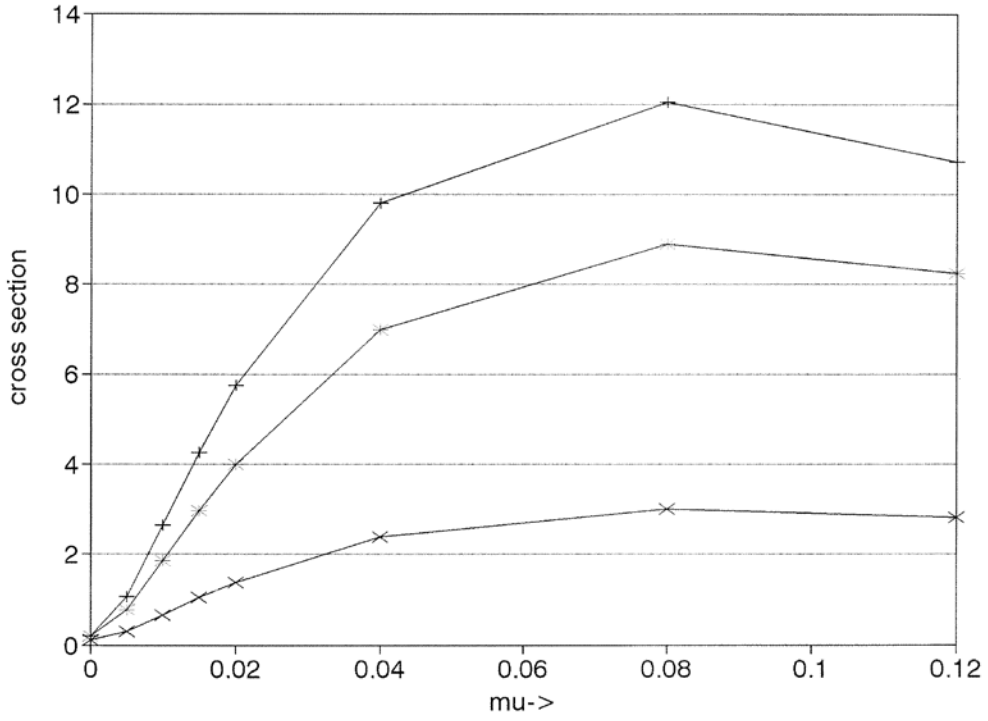

Fig.4 (color online only)TCS vs μ for triplet, k=0.5. The upper curve is for (l=0), the middle curve is for l=1 and the lowest one is for l=-1.

Fig. 4 exhibits similar behavior for the triplet state for k_i=0.5 as noted for the singlet one (vide Fig. 3).

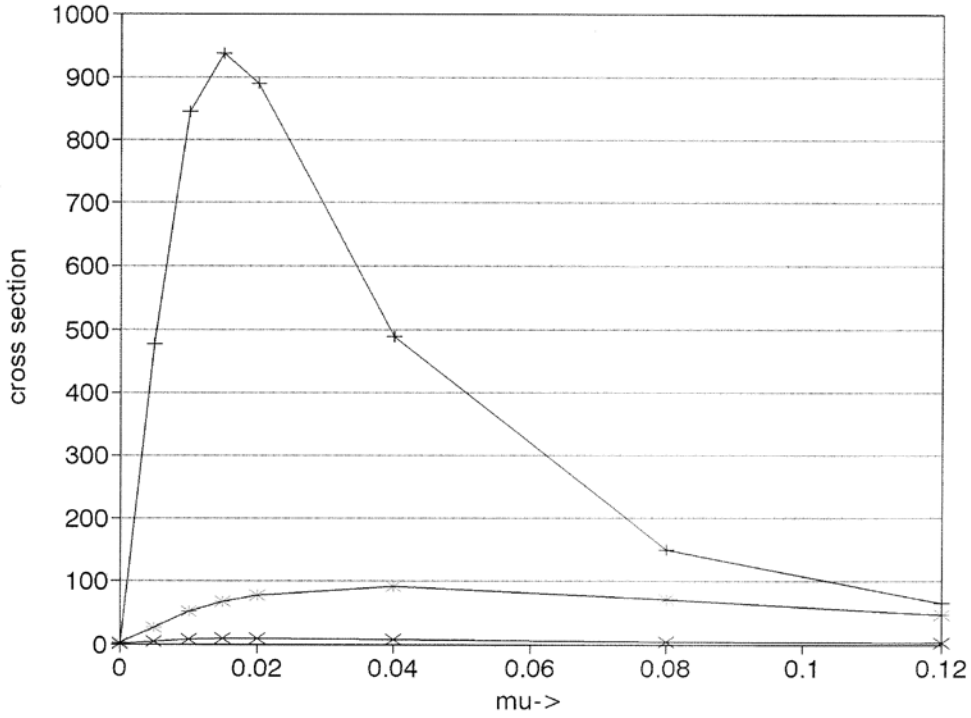

Figures 5a &5b: (color online only)Total singlet (5a) and triplet (5b) cross sections(TCS) in atomic unit (a.u.) against momentum k in (a.u.). The upper curve is for no photon exchange (l=0) , middle curve is for single photon absorption (l=+1) and the lowest is for the emission (l=-1) .

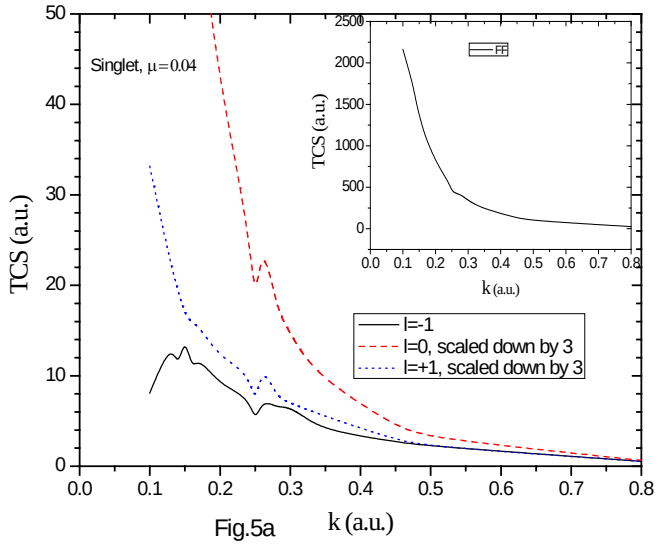

Fig.5a

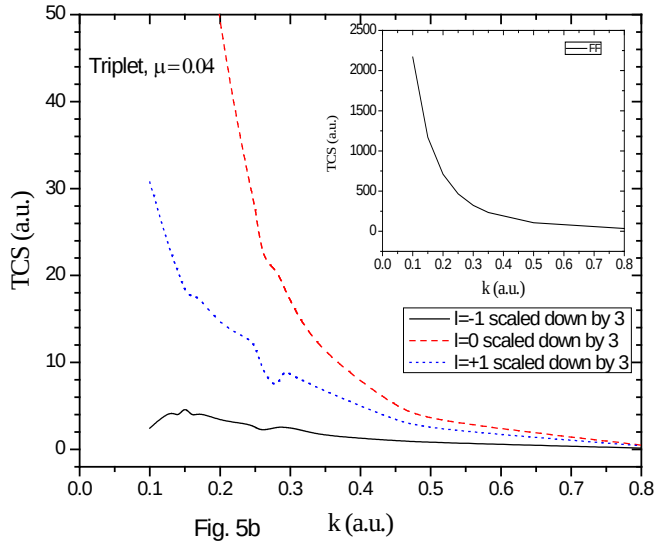

Fig. 5b

Figures 5 (a & b) exhibit a comparative study of the different laser assisted TCS ($l = 0,\pm1$) against the incident energy for both the singlet (Fig. 5a) and triplet states (Fig.5b) at $\mu = 0.04$. As may be noted from the Tables (I & II) as well as from Figs 6, the laser assisted TCS (for $l = 0,\pm1$) are highly suppressed w.r.t. the FF (5 – 6 times) for all values of μ, the suppression being increased with increasing incident energy for higher μ (e.g., μ =0.04) while for lower μ, the reverse is true , i.e., the degree of suppression

w.r.t. the FF decreases with increasing incident energy. On the contrary, the difference between the single photon absorption or emission $(l = \pm 1)$ and the no photon exchange ($l = 0$)TCS decreases with increasing incident energy. The no photon exchange cross sections ($l = 0$) dominates throughout the energy range over the other two ($l = \pm 1$) for all values of μ except for $\mu = 0$ where the single photon absorption (l=+1) dominates.

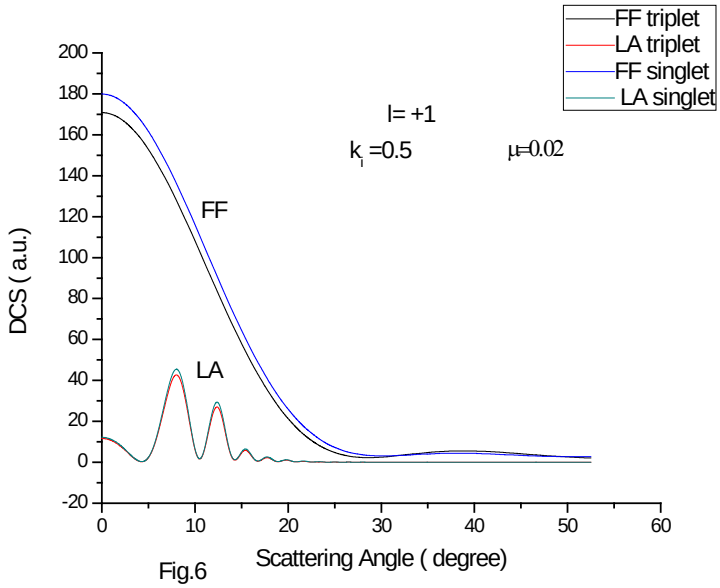

Fig.6

Fig.6 (color online only) Singlet and Triplet DCS for the parameters k_i =0.5, μ =0.02 and l=+1 along with the correspondind field free (FF) DCS.

Finally , we present some differential cross sections (DCS) for both the singlet and triplet along with their corresponding field free (FF) results for $k_i = 0.5$ and $\mu = 0.02$. Strong modification is noted in the laser assisted DCS as compared to the FF both quantitatively (suppression) and qualitatively for both the states with singlet all through lying slightly above the triplet. The oscillations noted in the LA DCS could be attributed to the oscillations of the Bessel functions ocurring in the expression of DCS (vide eqn.(19)).

Conclusions:

1. The presence of the Debye-Hückel potential ($\mu > 0$) enhances the cross sections in all cases (l=-1, 0, and 1) and for all values of the incident momentum. Apart from the qualitative modifications, the major quantitative effect of the external laser field is to suppress the field free cross sections. A significant difference is noted for the singlet and triplet cross sections. The suppression is much more in the triplet states.

2. Total cross sections decrease with the increase of the incident electron momentum and also with the increase of the Debye parameter as expected.

3. The DCS exhibit a number of oscillations at higher scattering angles that could be attributed to the oscillations in the Bessel function.

References:

1**.** S Chakraborty and Y.K. Ho, Phys. Rev A **77**,014502 (2008).

2. S Paul and Y.K.Ho, Physics of Plasmas **17,** 082704 (2010).

3. A. Ghoshal andY. K. Ho, Euro.Phys. J. D **55**, 581 (2009).

4. B. L. Whitten, N.F.Lane, J.C.Weisheit, Phys. Rev A **29**, 945 (1984).

5. R.S. Pundir and K.C. Mathur, J.Phys. B **17**, 4245 (1984).

6. G.J. Hatton, N.F.Lane and J.C.Weisheit , J.Phys.B **14**, 4879 (1981).

7. B.N. Chichikov, J.Phys. B **23,** L103 (1990).

8. A. Chattopadhyay and C Sinha, J. Plasma Fusion Res. **7**, 286 (2006).

9. Y. Chen, Phys. Rev. A **84**, 043423 (2011).

10. M.B.S. Lima , C.A.S.Lima and L.C.M. Mirande Phys. Rev.A **19**, 1796 (1979).

11. F. Brunel, Phys. Rev. Lett., **59**, 52 (1987).

12. A. Weingartshofer , J.K.Holmes,G.Caudle and E.M.Clarke, Phys. Rev.Lett. **39**, 269 (1977).

13. A. Weingartshofer , J.K.Holmes, G.Caudle and E.M. Clarke, Phys. Rev A **19**, 2371 (1979).

14. N.J. Mason, Rep. Prog. Phys. **56**, L275 (1993).

15. B. Wallbank & J.K. Holmes, J. Phys. B **29**, 5881 (1996).

16. M.O. Musa, A McDonald, L.Tidswell, J Holmes and B. Wallbank, J. Phys. B **43**, 175201 (2010).

17. C. Sinha and A. K. Bhatia, Phys. Rev. A **83**, 063417 (2011).

18. P. Debye and E. Hückel, Physik. Z., **24**, 185 (1923).

19. N. M. Kroll and K. M. Watson, Phys. Rev. A **8**, 804 (1973).

20. A. Chattopadhyay and C. Sinha, J. Phys. B **37**, 3283 (2004).

21. A. Chattopadhyay and C. Sinha, Phys. Rev A **72**, 053406 (2005).

22. A. K. Bhatia and A. Temkin, Phys. Rev. A **64**, 032709 (2001).

23. A. Temkin and Lamkin, Phys. Rev. **121**, 788 (1961).

24. A. K. Bhatia, Phys. Rev. A **75**, 032713 (2007).